PFISR Science: The First Three Years

Joshua Semeter (co-Chair)
Bill Bristow (co-Chair)
John Meriwether
David Hysell
David Knudsen
Donald Hampton
Mark Conde
Shasha Zou
Jonathan Sparks
Thomas Butler
John Foster
Miguel Larsen
Jun Liang
Larry Lyons
Kathryn McWilliams
Robert Michell
Marilia Samara
Ingemar Haggstrom
Johnathan Burchill
Michael Nicolls
Richard Collins
Toshi Nishimura
Tony van Eyken
Robert Robinson
Kristina Lynch
Frederick Wilder
Rich Behnke
Antonius Otto
Farzad Kamalabadi
Syun-Ichi Akasofu
Roger Smith
Craig Heinselman

Poker Flat Incoherent Scatter Radar (PFISR)

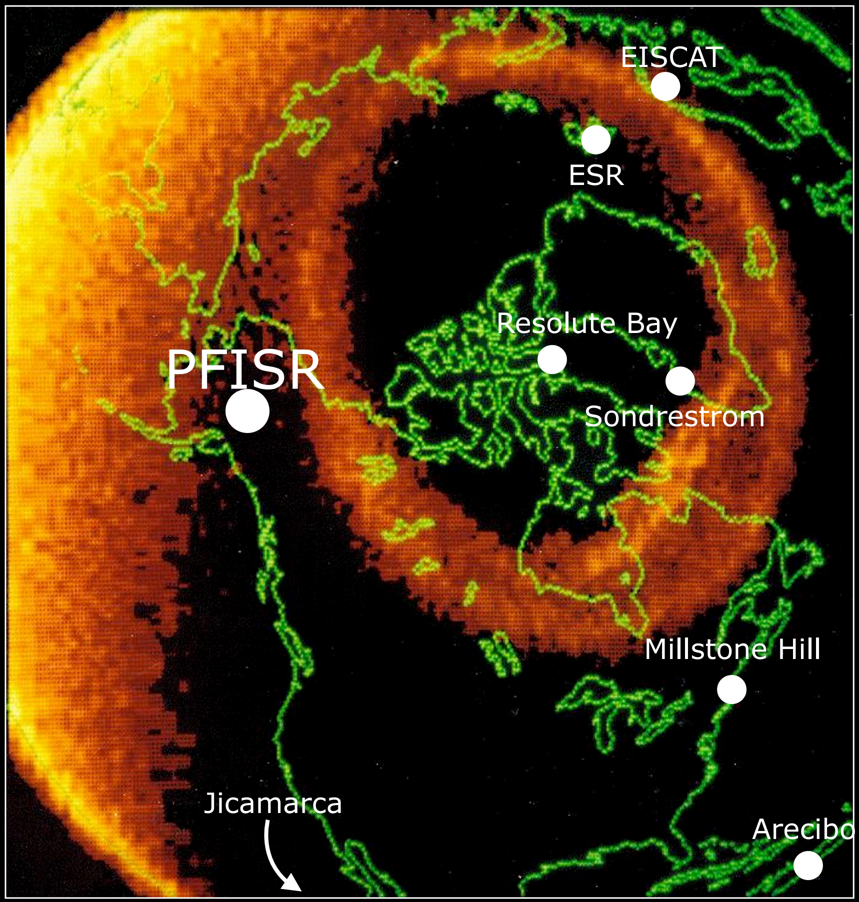

Poker Flat, Alaska

How does a Doppler radar work?

Two key concepts:

Distant ⟺ Time

$$R = c\Delta t/2$$

Velocity ⟺ Frequency

$$v = -f_D\lambda_0/2$$

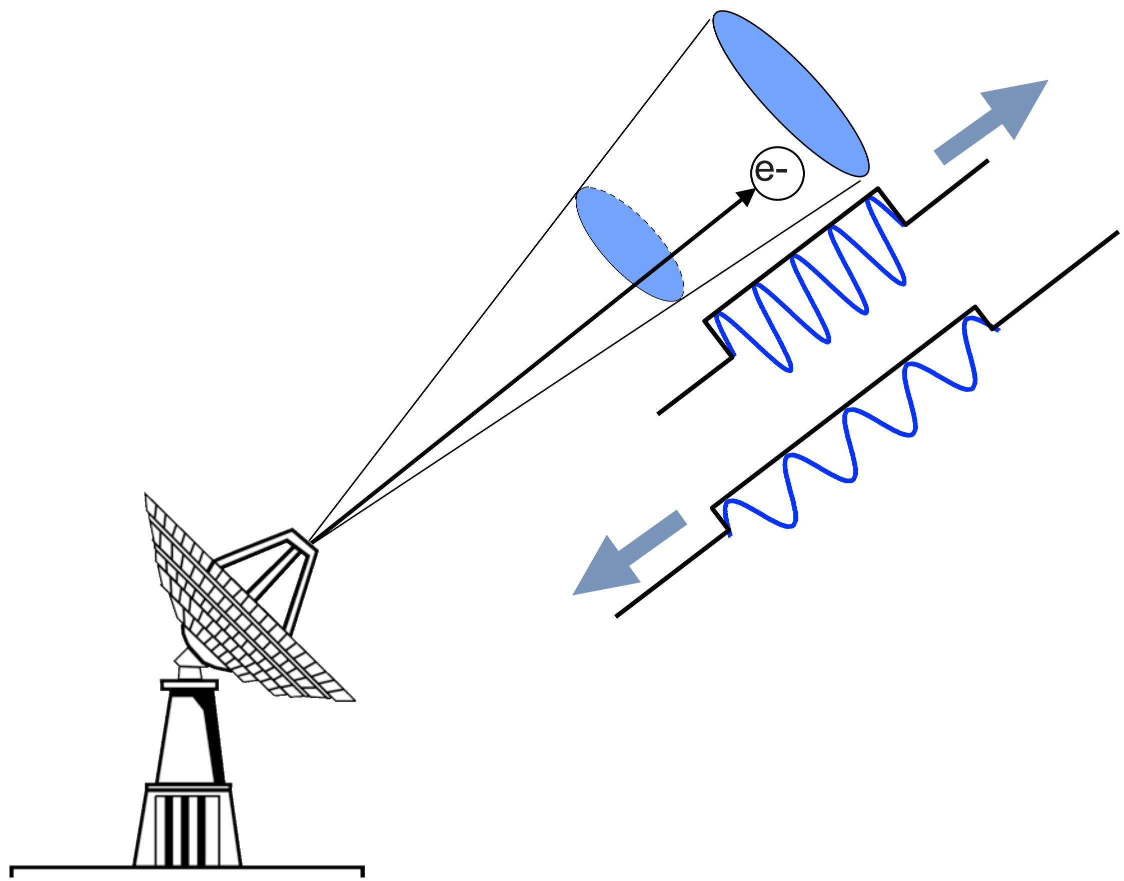

A Doppler radar measures backscattered power as a function range and velocity. Velocity is manifested as a Doppler frequency shift in the received signal.

How does a Doppler radar work?

Two key concepts:

Distant ⟺ Time

$$R = c\Delta t/2$$

Velocity ⟺ Frequency

$$v = -f_D \lambda_0 / 2$$

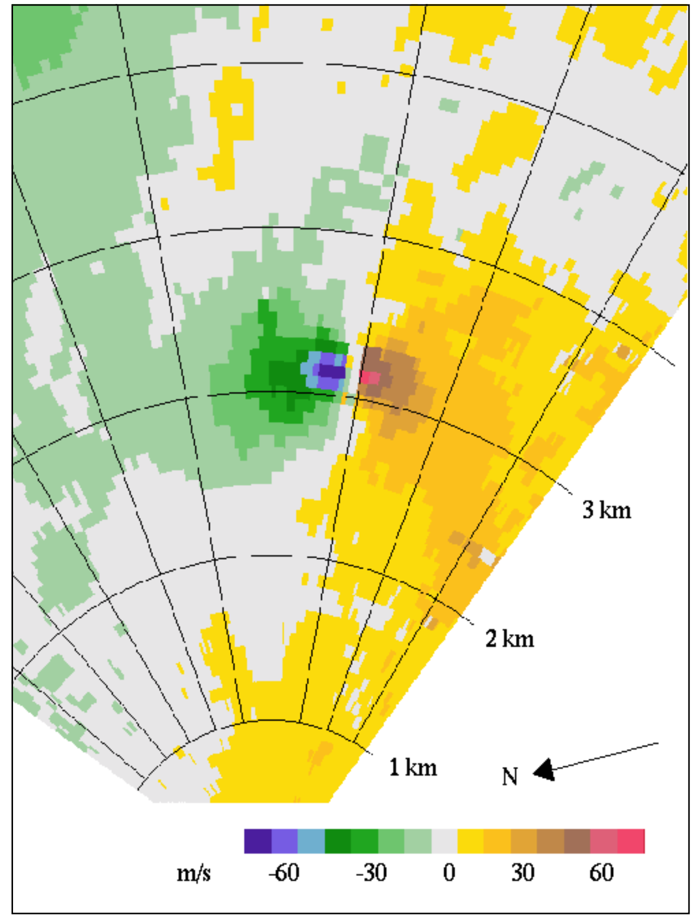

A Doppler radar measures backscattered power as a function range and velocity. Velocity is manifested as a Doppler frequency shift in the received signal.

How does a Doppler radar work?

Two key concepts:

Distant ⟺ Time

$$R = c\Delta t/2$$

Velocity ⟺ Frequency

$$v = -f_D \lambda_0/2$$

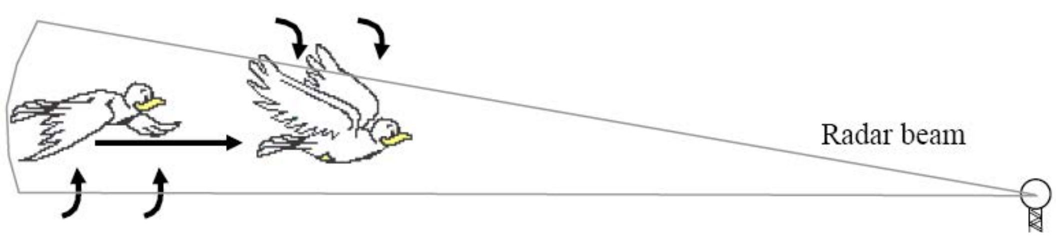

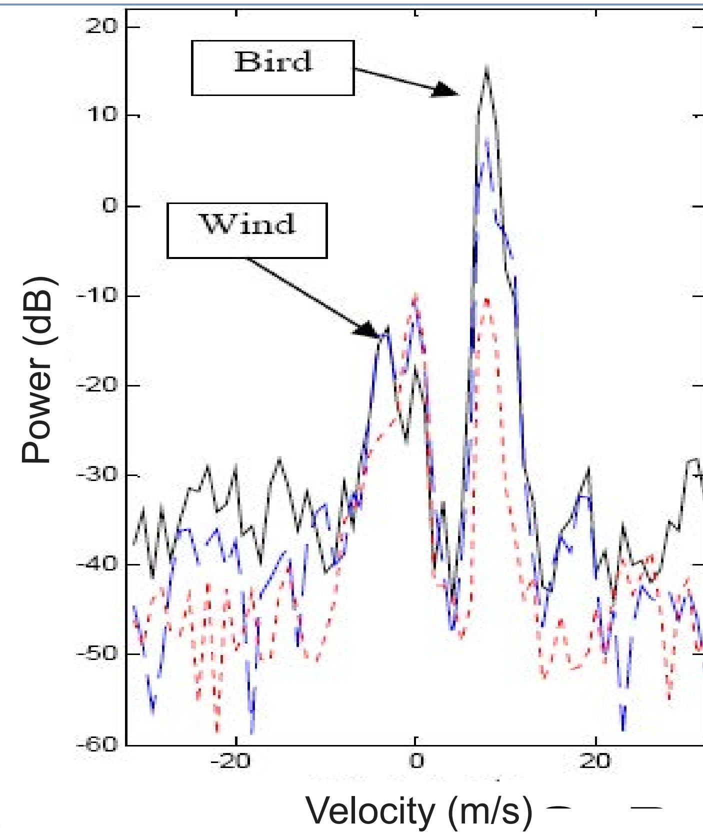

If there is a distribution of targets moving at different velocities (e.g., electrons in the ionosphere) then there is no single Doppler shift but, rather, a Doppler spectrum.

What is the Doppler spectrum of the ionosphere at UHF (λ of 10 to 30 cm)?

Plasma simulation

Particle-in-cell (PIC):

$$\frac{d\,\mathbf{v}_i}{d\,t} = \frac{q_i}{m_i}(\mathbf{E}(\mathbf{x}_i) + \mathbf{v}_i \times \mathbf{B}(\mathbf{x}_i))$$

$$\nabla \times \mathbf{E} = \frac{-\partial \mathbf{B}}{\partial t}$$

$$\nabla \times \mathbf{B} = \mu_0 \mathbf{J} + \frac{1}{c^2}\frac{\partial \mathbf{E}}{\partial t}$$

$$\nabla \cdot \mathbf{E} = \frac{\rho}{\epsilon_0}$$

$$\nabla \cdot \mathbf{B} = 0$$

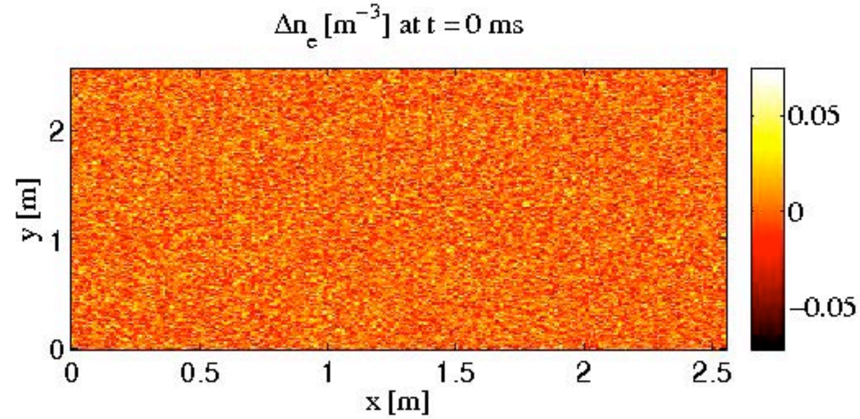

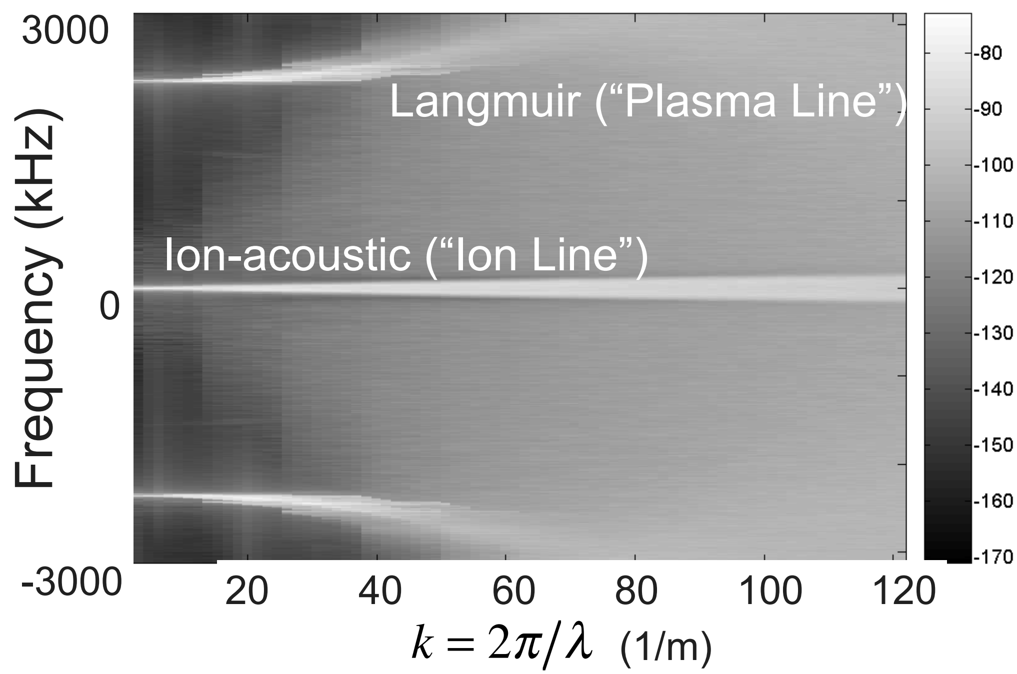

Simple rules yield complex behavior

ISR measures a cut through this surface at a particular wave number

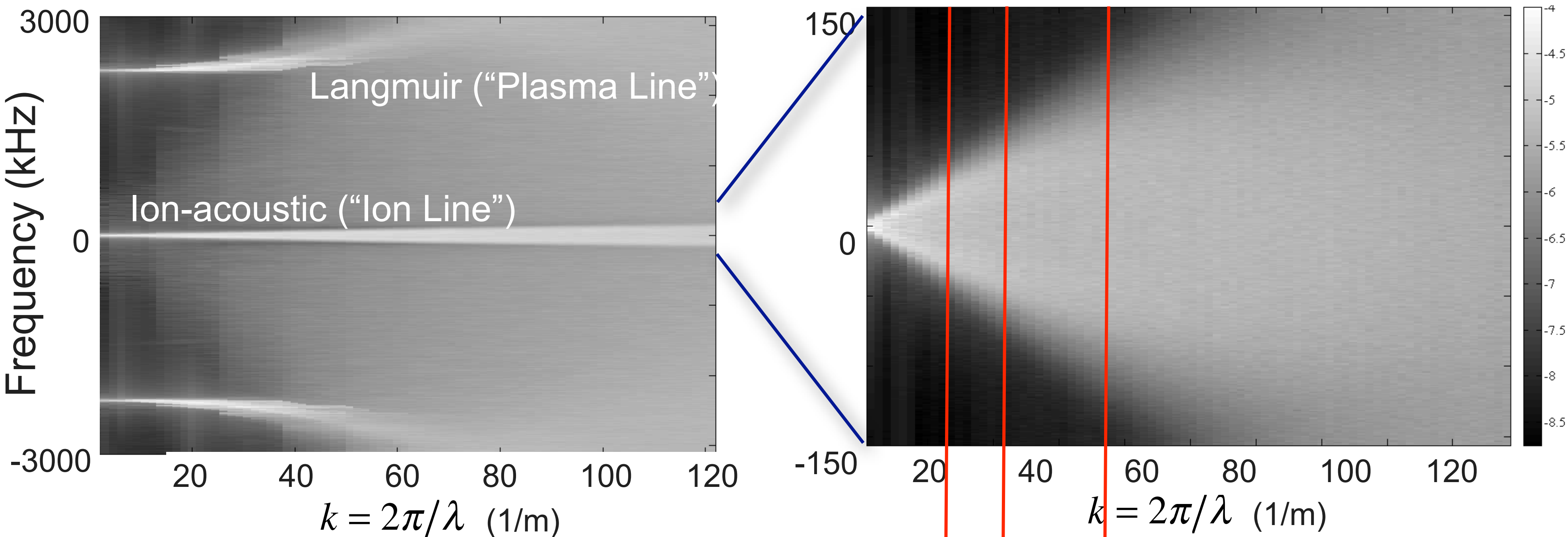

Ion-acoustic "lines" are broadened by Landau damping

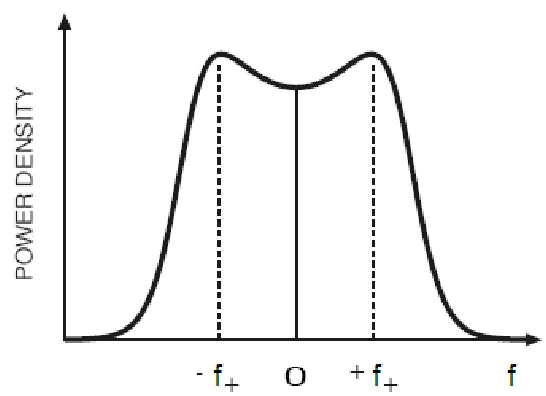

Exact expression for the radar cross section of the ionosphere at UHF

$$\sigma(\omega) = \frac{\left| 1 + \left(\frac{\lambda}{4\pi}\right)^2 \sum_1 \left(\frac{1}{D_i}\right)^2 F_i(\omega)\right|^2 \overline{\left|N_e^0(\omega)\right|^2} + \left(\frac{\lambda}{4\pi D_e}\right)^4 \left|F_e(\omega)\right|^2 \sum_i \overline{\left|N_i^0(\omega)\right|^2}}{\left| 1 + \left(\frac{\lambda}{4\pi}\right)^2 \left\{\left(\frac{1}{D_e}\right)^2 \cdot F_e(\omega) + \sum_i \left(\frac{1}{D_i}\right)^2 F_i(\omega)\right\}\right|^2}$$

where:

$$F_e(\omega) = 1 - \omega\int_o^\infty \exp\left(-\frac{16\pi^2 KT_e}{\lambda^2 m_e}\tau^2\right)\sin(\omega\tau)\,d\tau - j\omega\int_0^\infty \exp\left(-\frac{16\pi^2 KT_e}{\lambda^2 m_e}\tau^2\right)\cos(\omega\tau)\,d\tau$$

$$F_i(\omega) = 1 - \omega\int_o^\infty \exp\left(-\frac{16\pi^2 KT_i}{\lambda^2 m_i}\tau^2\right)\sin(\omega\tau)\,d\tau - j\omega\int_0^\infty \exp\left(-\frac{16\pi^2 KT_i}{\lambda^2 m_i}\tau^2\right)\cos(\omega\tau)\,d\tau$$

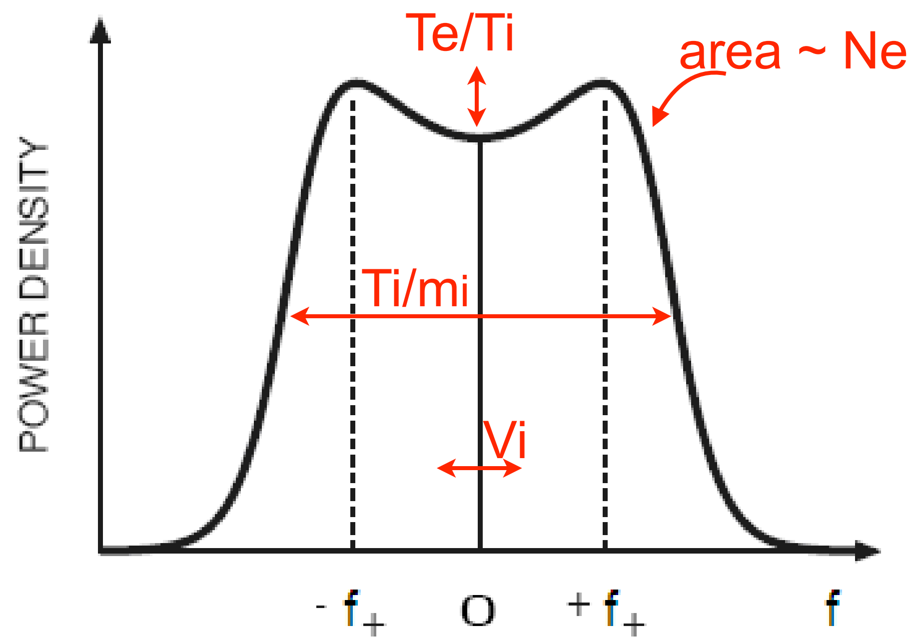

From Evans, IEEE Transactions, 1969

Incoherent averaging

Normalized ISR spectrum for different integration times at 1290 MHz

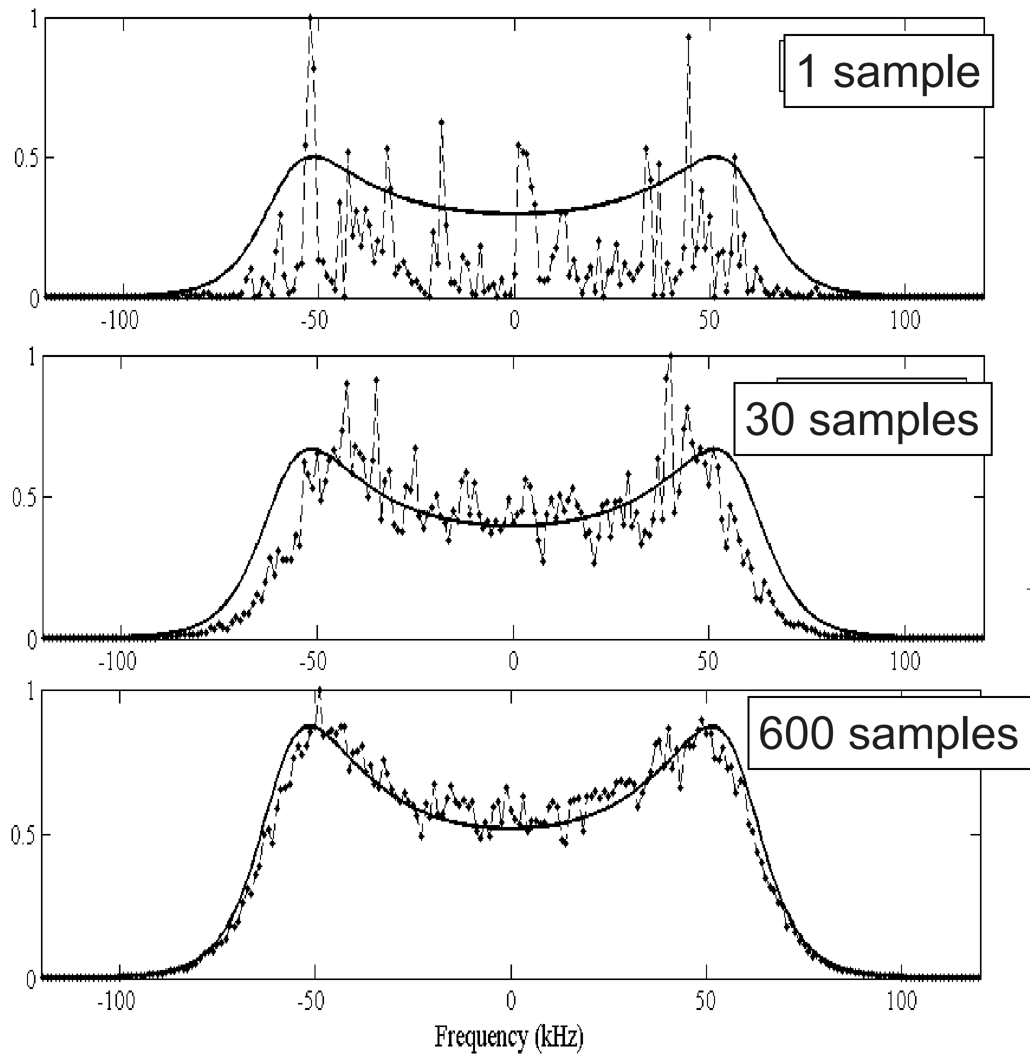

We are seeking to estimate the power spectrum of a Gaussian random process. This requires that we sample and average many independent "realizations" of the process.

$$\text{Uncertainties} \propto \frac{1}{\sqrt{\text{Number of Samples}}}$$

The auroral ionosphere

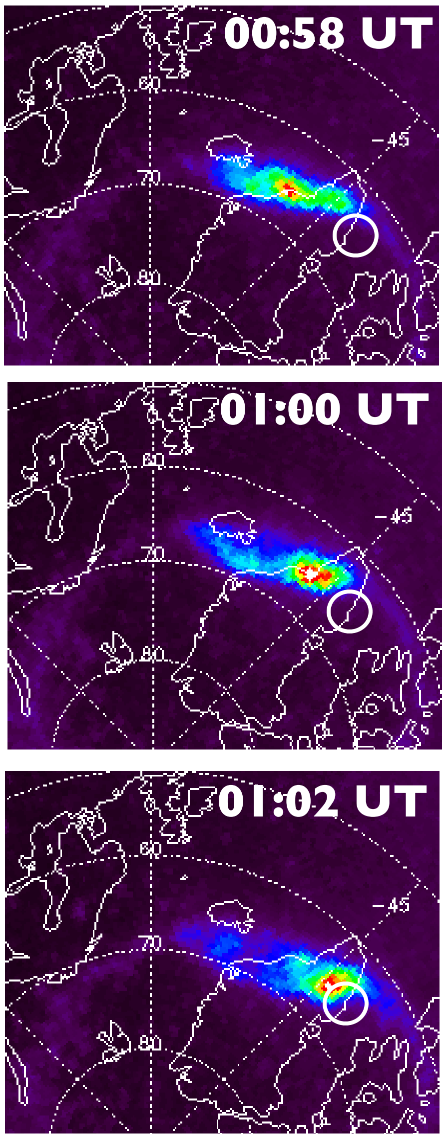

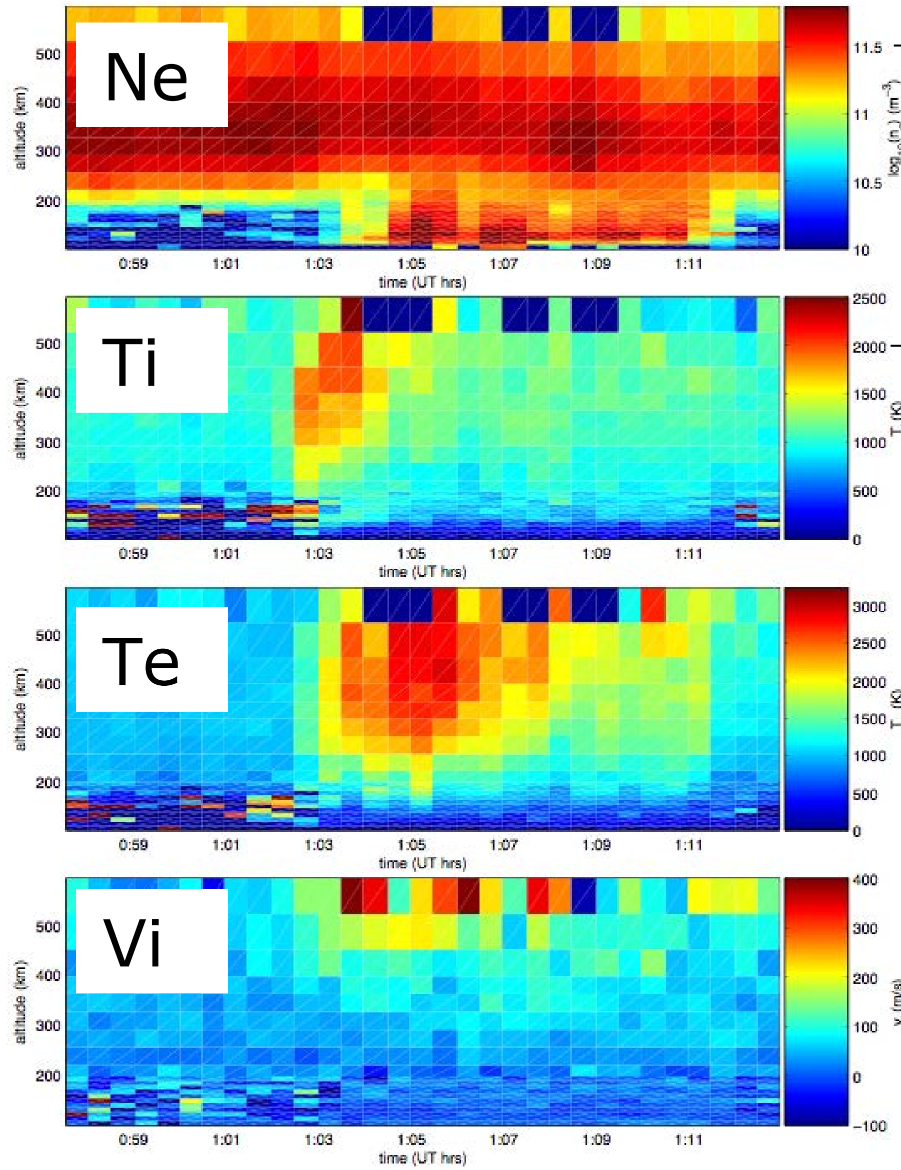

Sondrestrom ISR

Semeter et al., jgra 2005

Dish Versus Phased-array

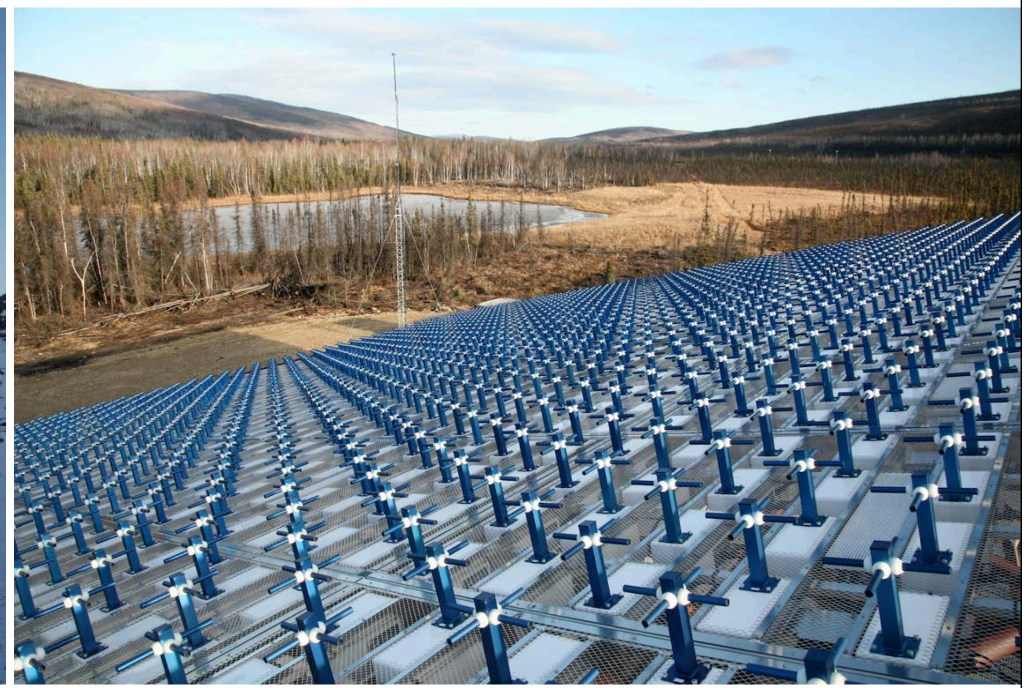

-FOV: Entire sky
-Integration at each position before moving
-Power concentrated at Klystron
-Significant mechanical complexity

-FOV: +/- 15 degrees from boresight
-Integration over all positions simultaneously
-Power distributed
-No moving parts

CIR heating of the auroral ionosphere

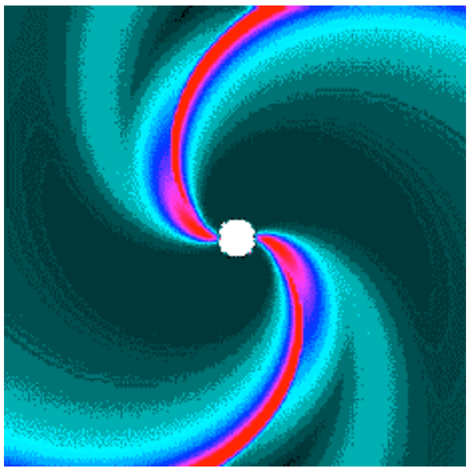

Corotating
Interaction
Region

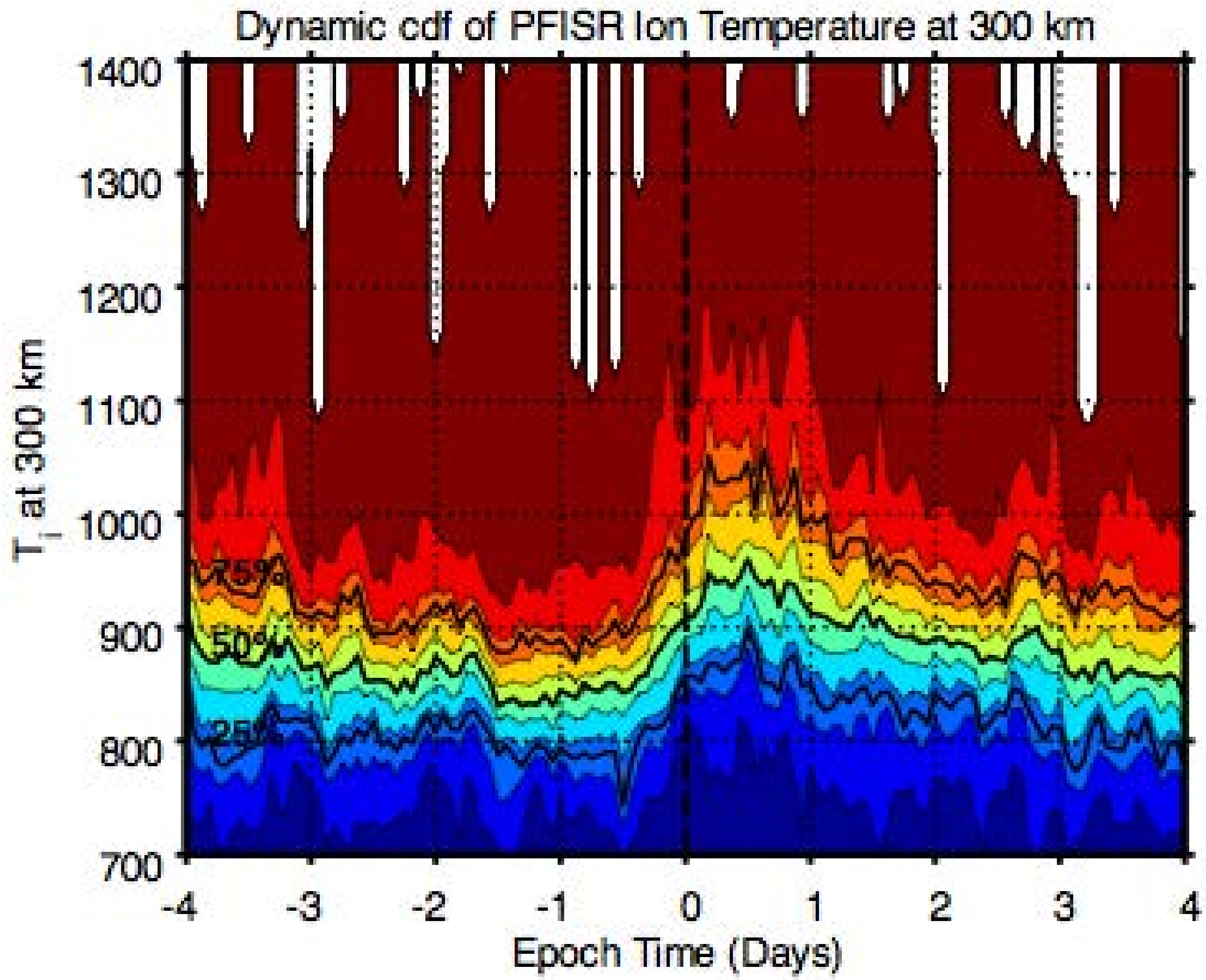

Sojka et al., GRL 2009.

3-D imaging of auroral ionization

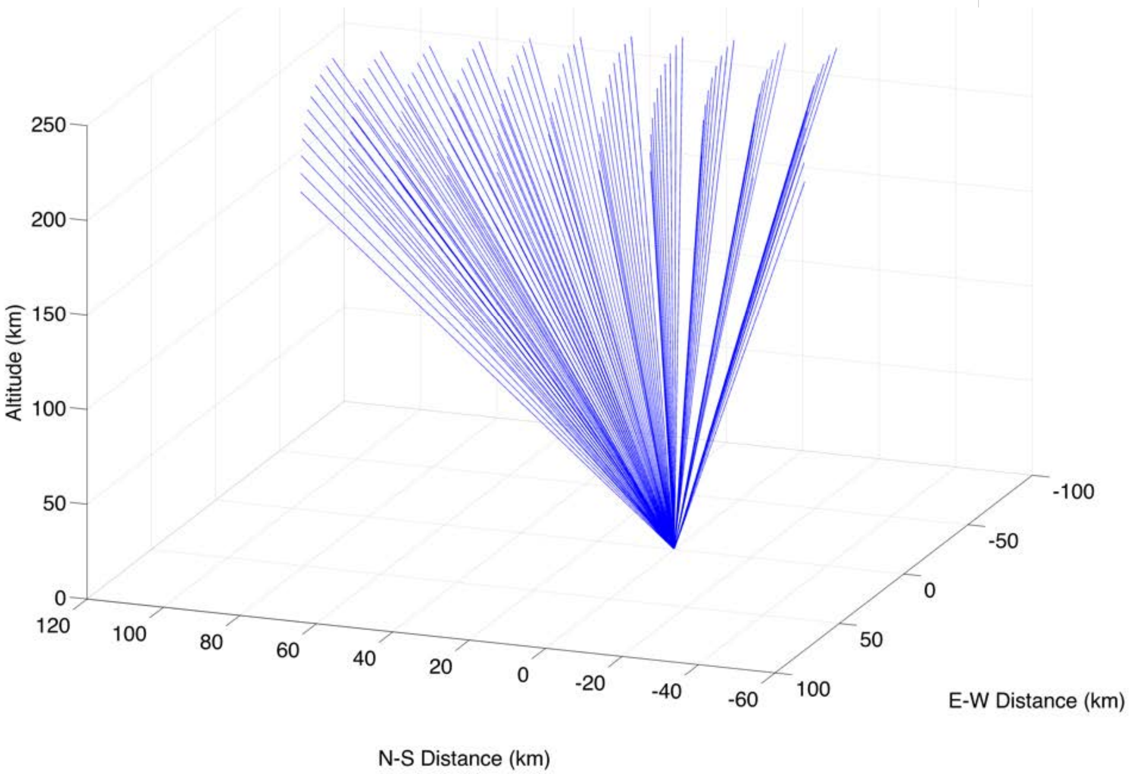

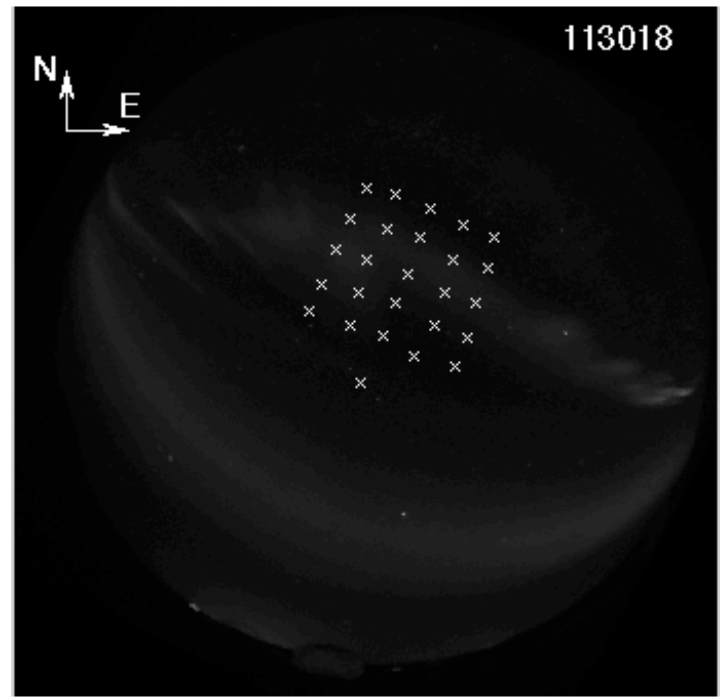

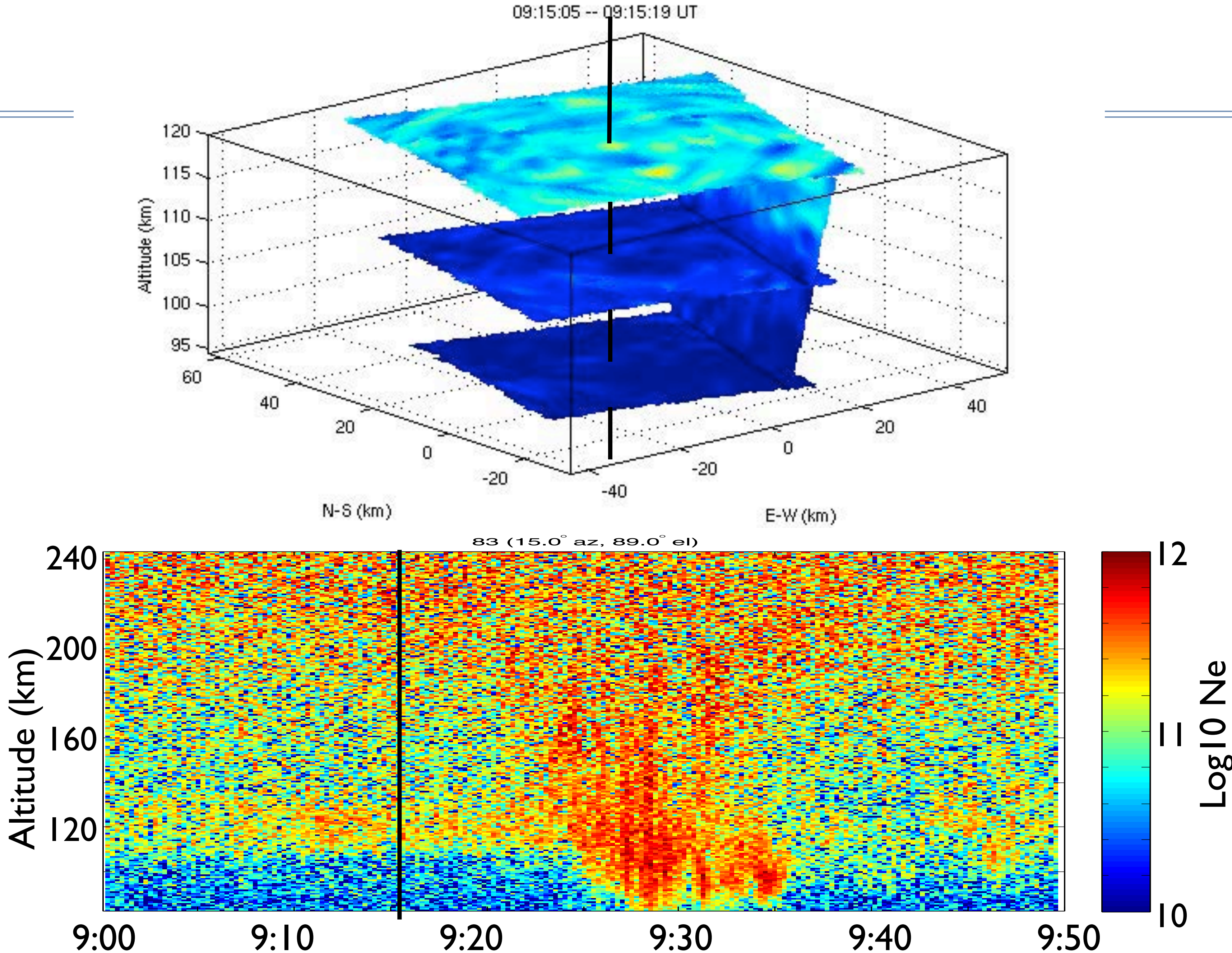
09:15:05 -- 09:15:19 UT
Altitude (km)
120
115
110
105
100
95
60
40
20
0
-20
N-S (km)
-40
-20
0
20
40
E-W (km)
83 (15.0° az, 89.0° el)
Altitude (km)
240
200
160
120
9:00
9:10
9:20
9:30
9:40
9:50
12
11
10
Log10 Ne

Multi-Instrument Measurements of Polar Mesospheric Clouds

Panoramic image of NLC display on 10-11, August, 2007.

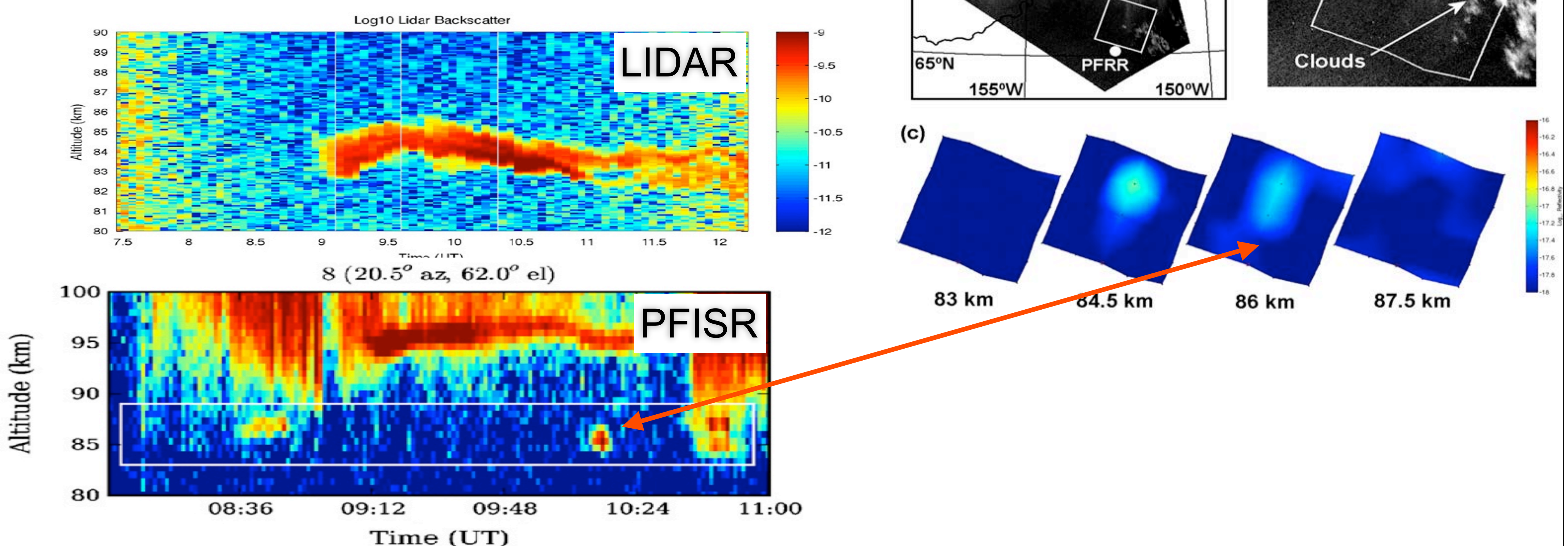

Taylor et al., JASTP 2009

2D Imaging of Convective Flows

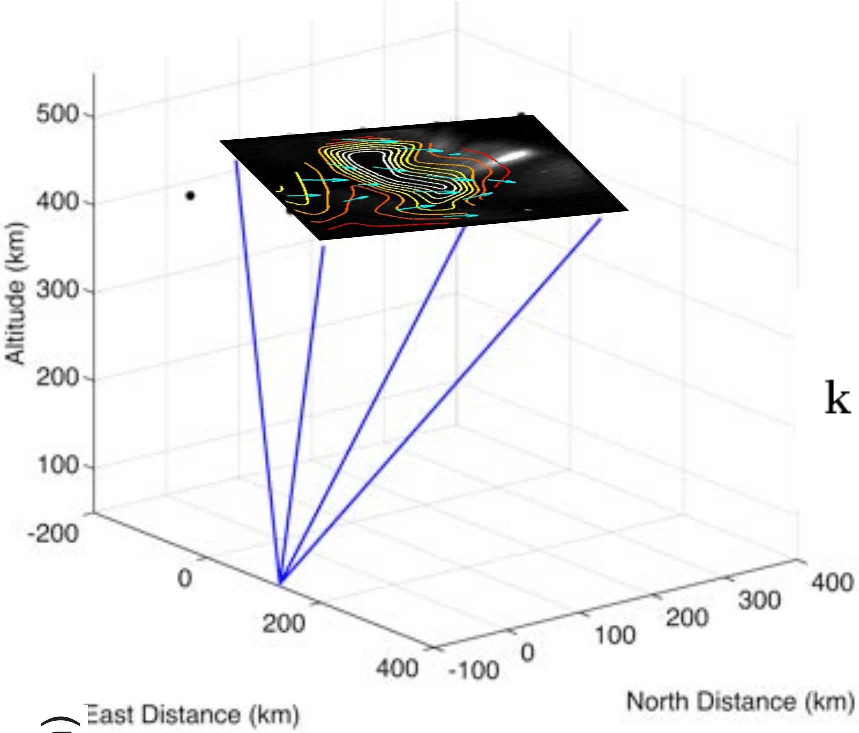

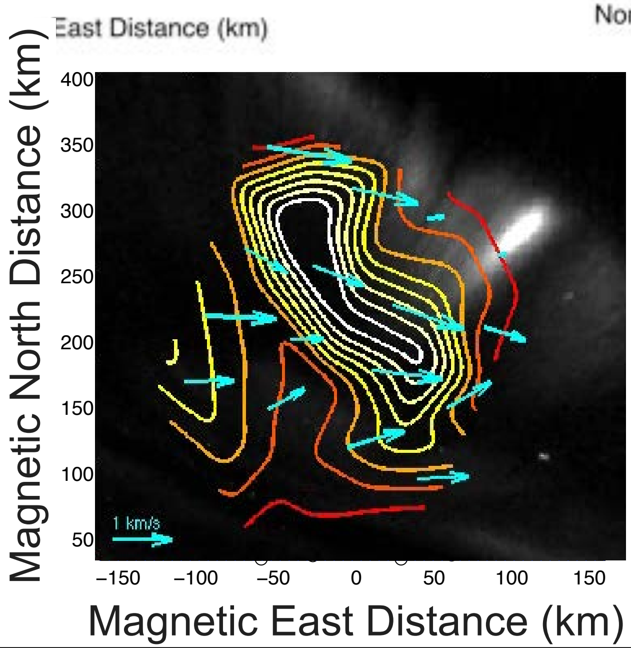

$$v_{los} = \mathbf{k} \cdot \begin{bmatrix} v_e & v_n & v_{\|} \end{bmatrix}^T$$

$$\mathbf{k} = \begin{bmatrix} \cos\theta \sin\phi \\ \cos\theta\cos\phi \\ \sin\theta \end{bmatrix}^T \begin{bmatrix} \cos\delta & \sin I \sin\delta & -\cos I \sin\delta \\ -\sin\delta & \cos\delta \sin I & -\cos I \cos\delta \\ 0 & \cos I & \sin I \end{bmatrix}$$

$$\begin{bmatrix} v_{los}^1 \\ v_{los}^2 \\ \vdots \\ v_{los}^i \\ \vdots \\ v_{los}^N \end{bmatrix} = \begin{bmatrix} \mathbf{k}^1 \\ \mathbf{k}^2 \\ \vdots \\ \mathbf{k}^i \\ \vdots \\ \mathbf{k}^N \end{bmatrix} \mathbf{v} + \begin{bmatrix} e_{los}^1 \\ e_{los}^2 \\ \vdots \\ e_{los}^i \\ \vdots \\ e_{los}^N, \end{bmatrix}$$

$$\mathbf{v}_{los} = A\mathbf{v} + \mathbf{e}_{los}$$

Semeter et al, JGRA 2010

The Harang Reversal Region and Substorm Onset

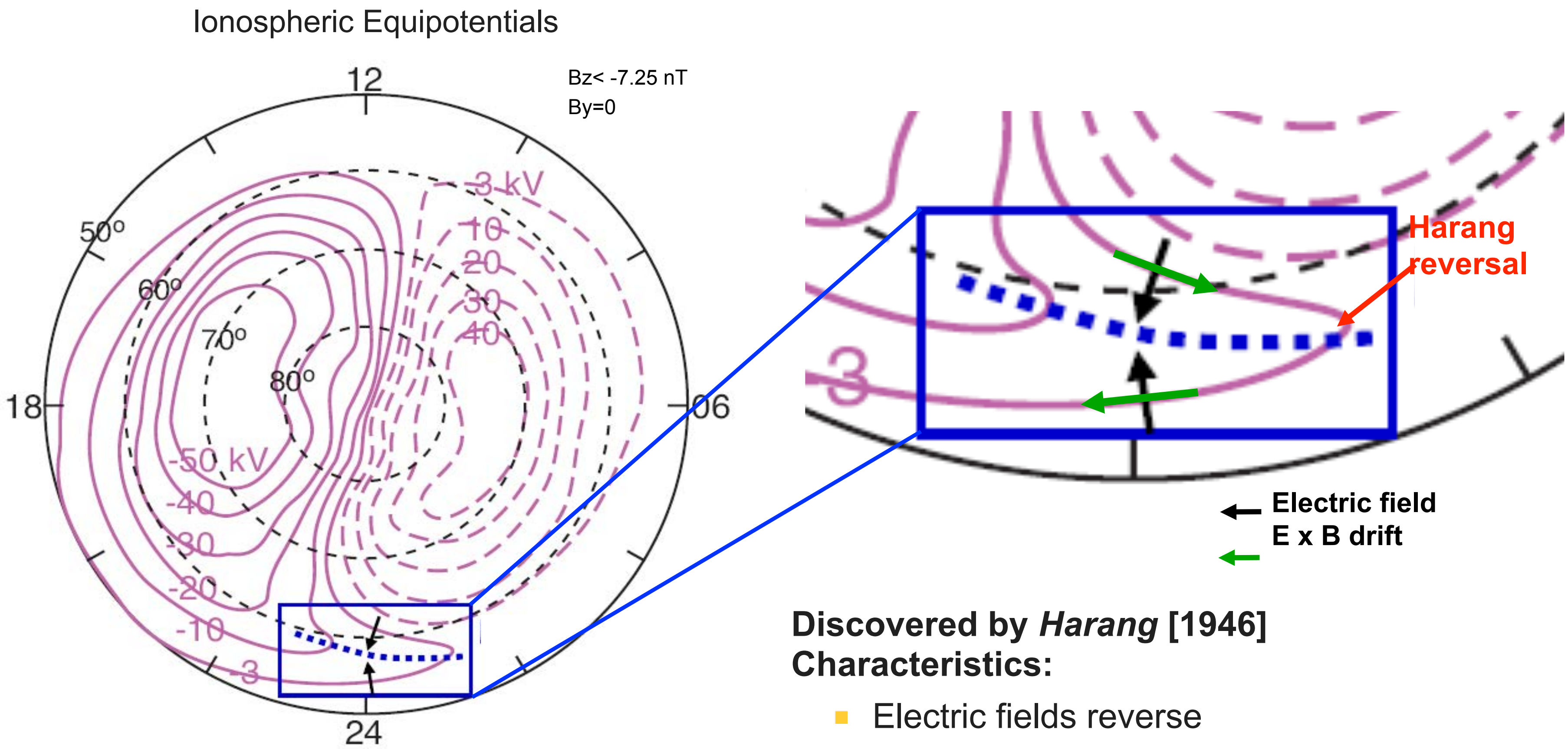

Based on Weimer, [1995]

Discovered by *Harang* [1946]
Characteristics:

- Electric fields reverse
- Flow shear
- Eastward and westward electrojets overlap

Zou et al., JGRA 2009; Lyons et al., JASTP 2009

Dynamic 2D flow fields and auroral forms

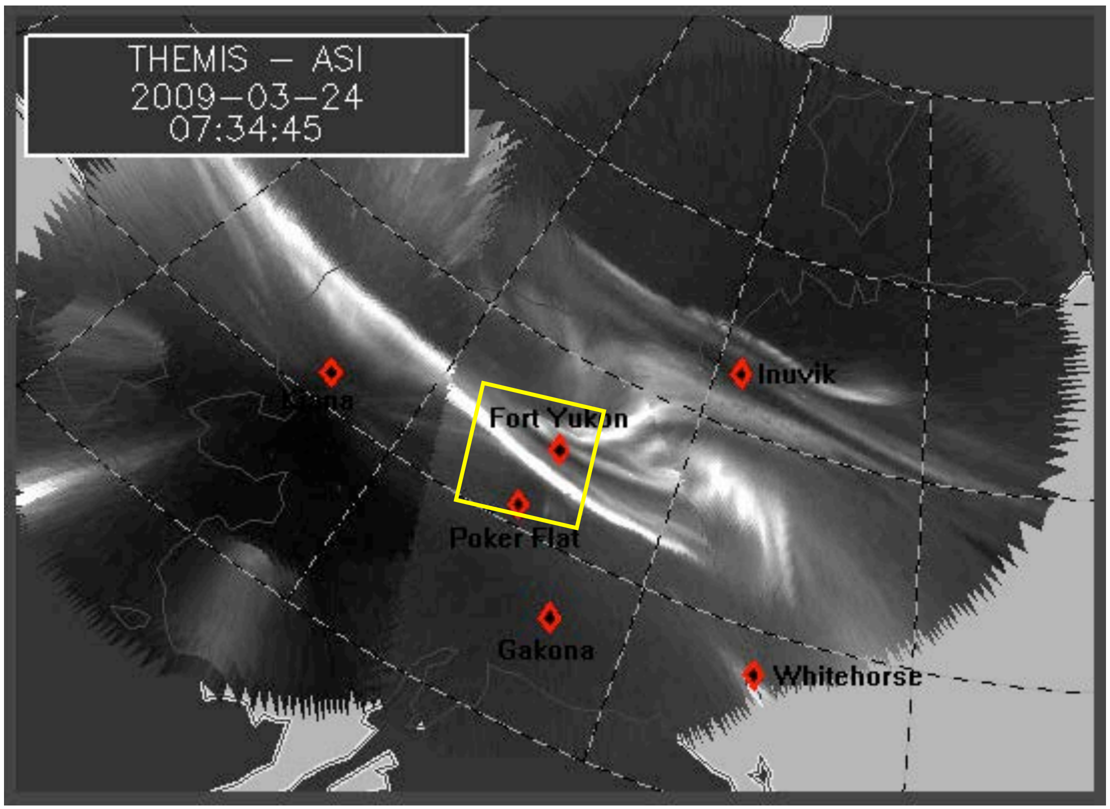

Courtesy Emma Spanswick and Eric Donovan

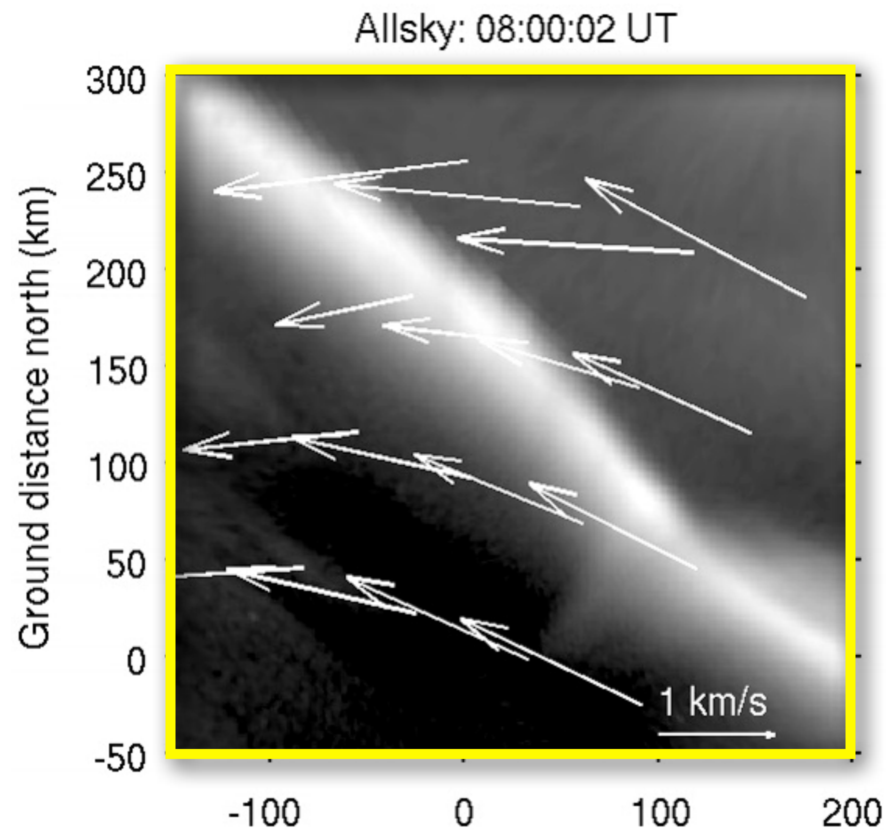

Zou et al., JGRA 2009; Lyons et al., JASTP 2009

Butler et al., RS 2010

Dynamic 2D flow fields and auroral forms

Semeter et al. (JGRA 2010), Butler et al. (RS 2010, in press)

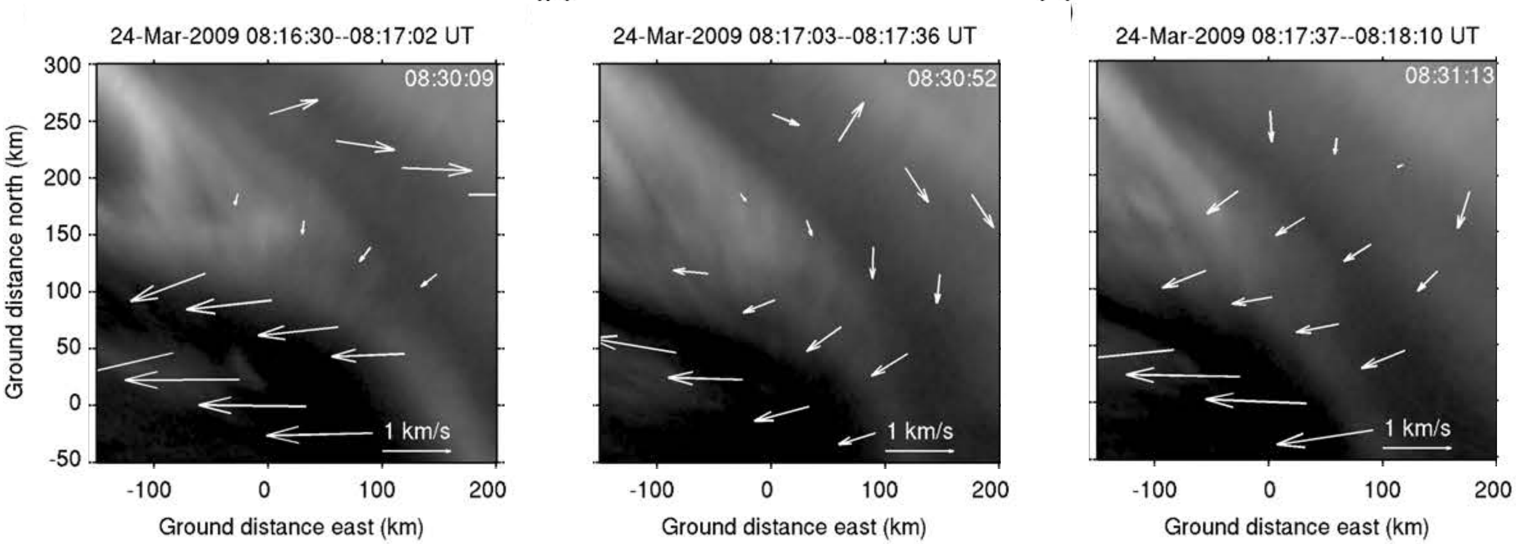

Plasma flow field confirms optical signature of Harang reversal

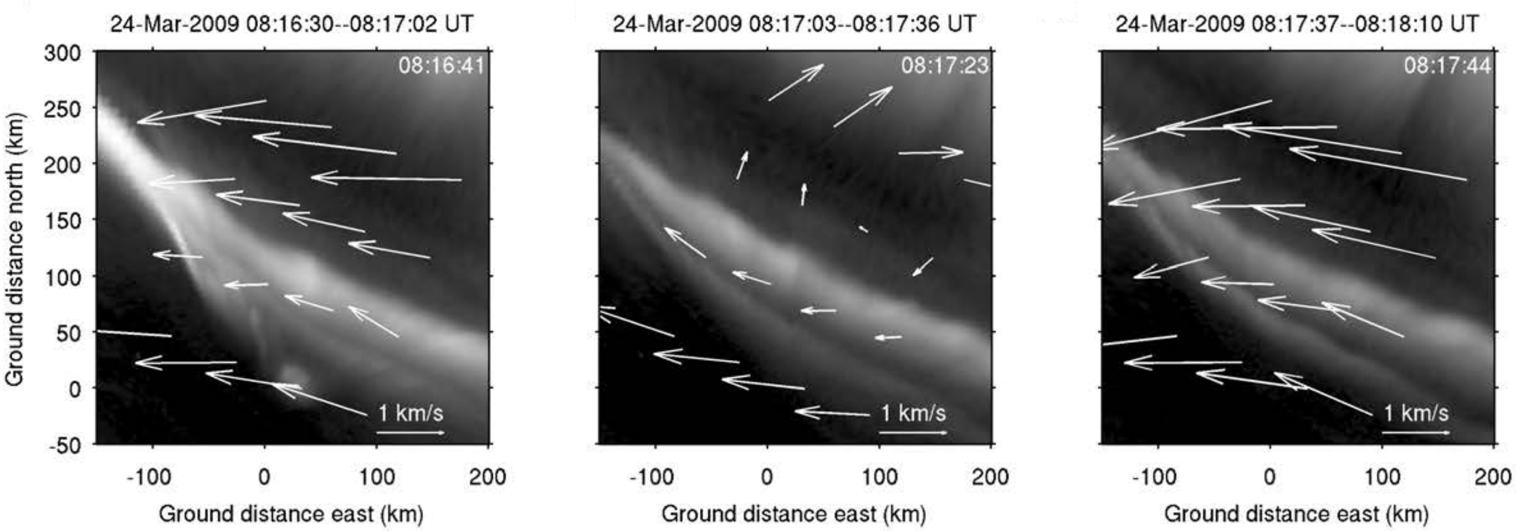

Rapid (~30-sec) coherent variations in flow also observed along "quiet" arc

Similar dynamic observed by Bristow et al. (JGRA 2008) with SuperDARN

PFISR Measurements of Winds and Waves in the D region

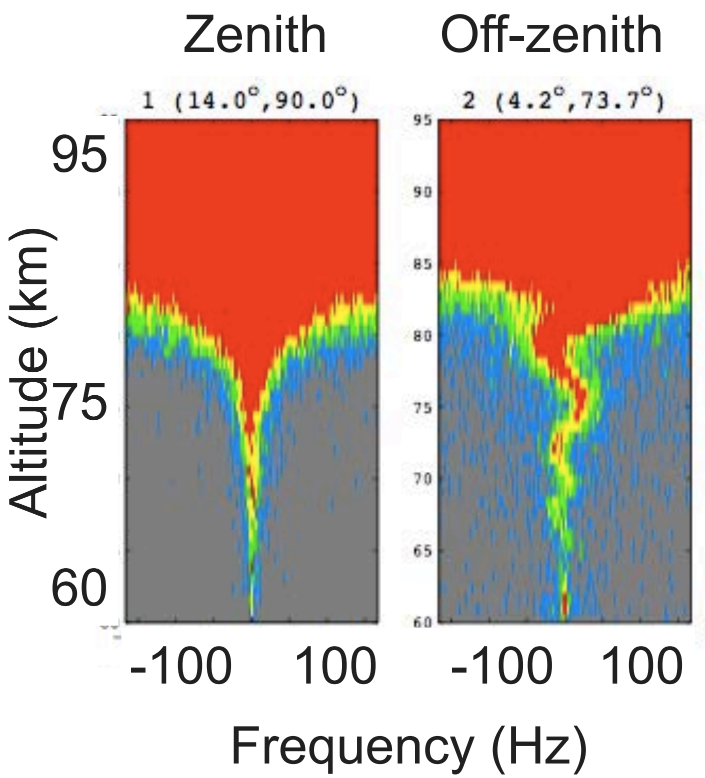

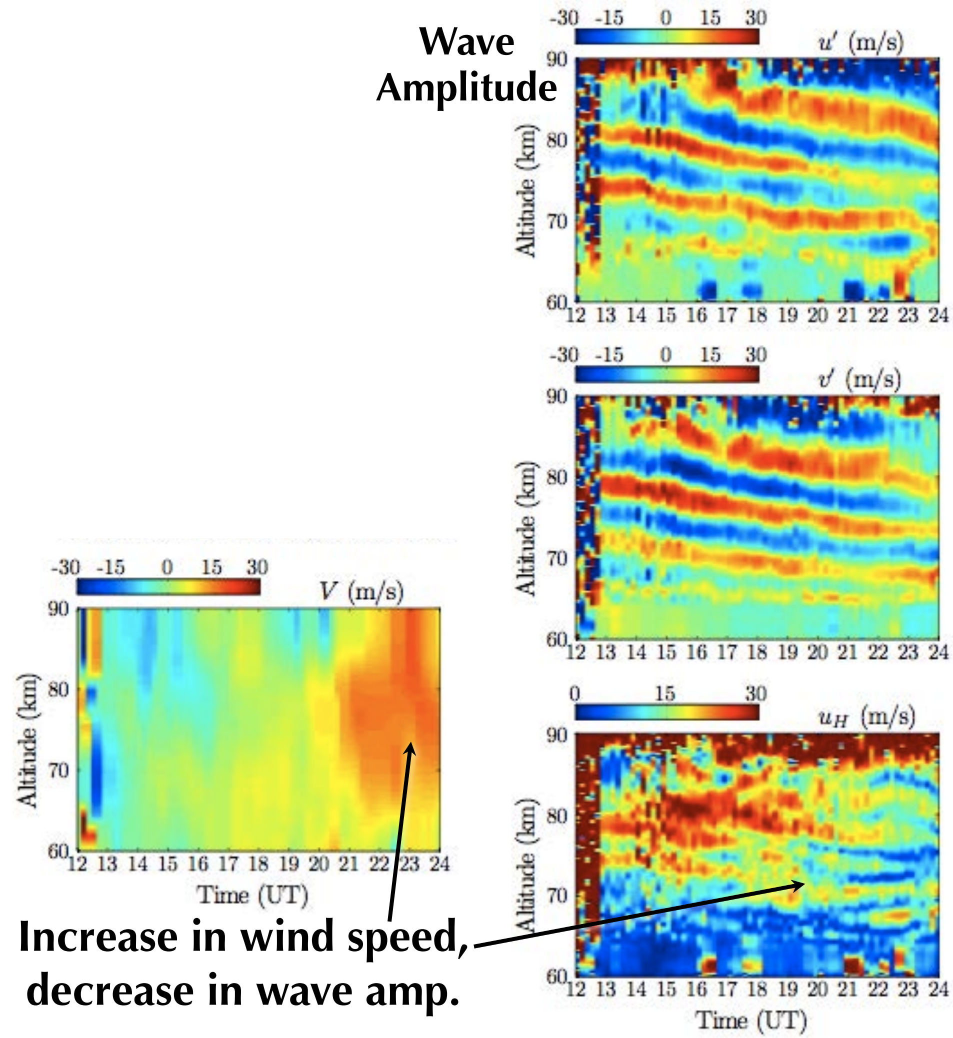

Nicolls et al., JGRA, 2010

Low altitude ionospheric turbulence

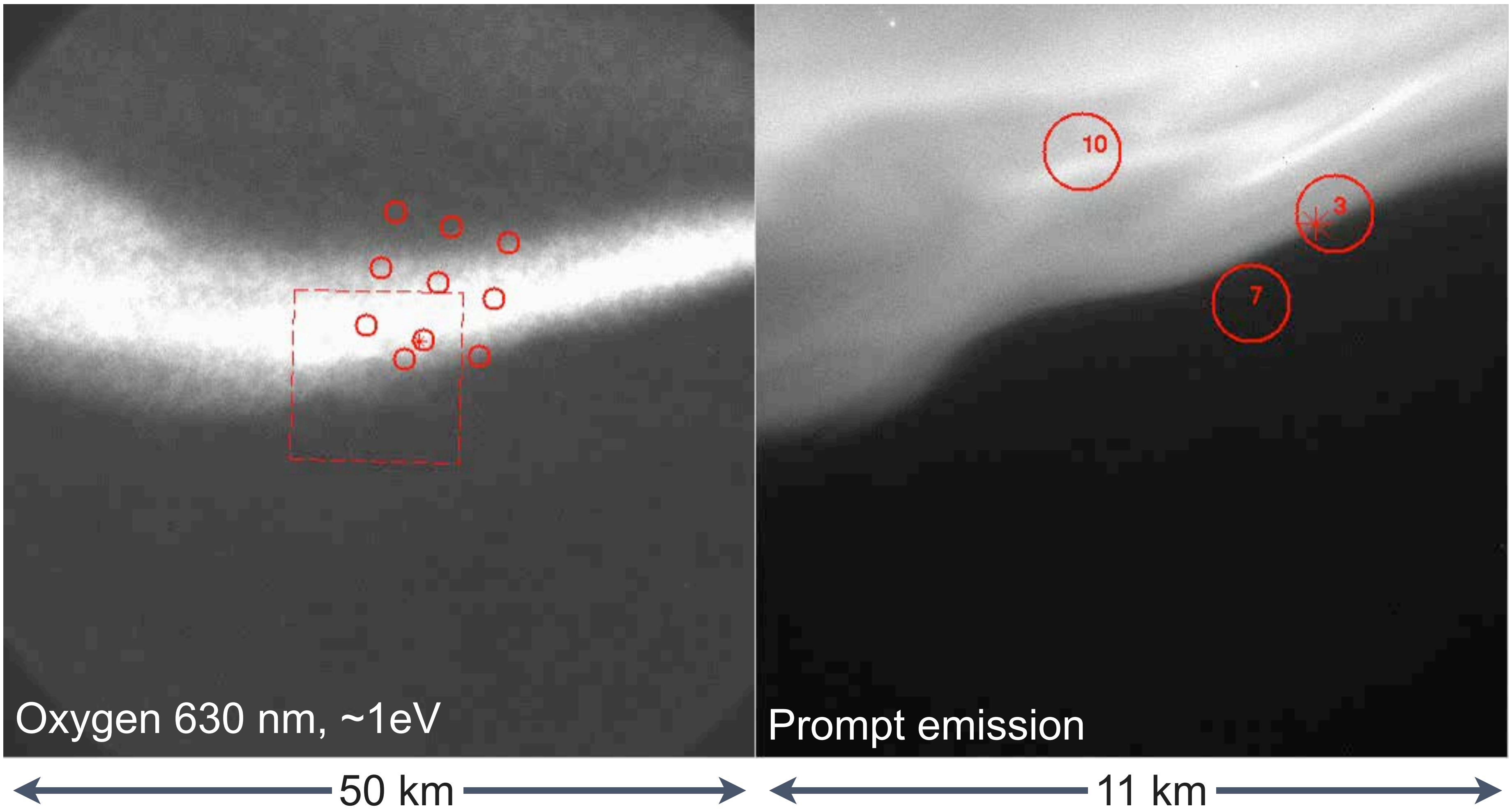

Semeter et al., GRL 2006, JGRA 2009

Non-thermal plasma

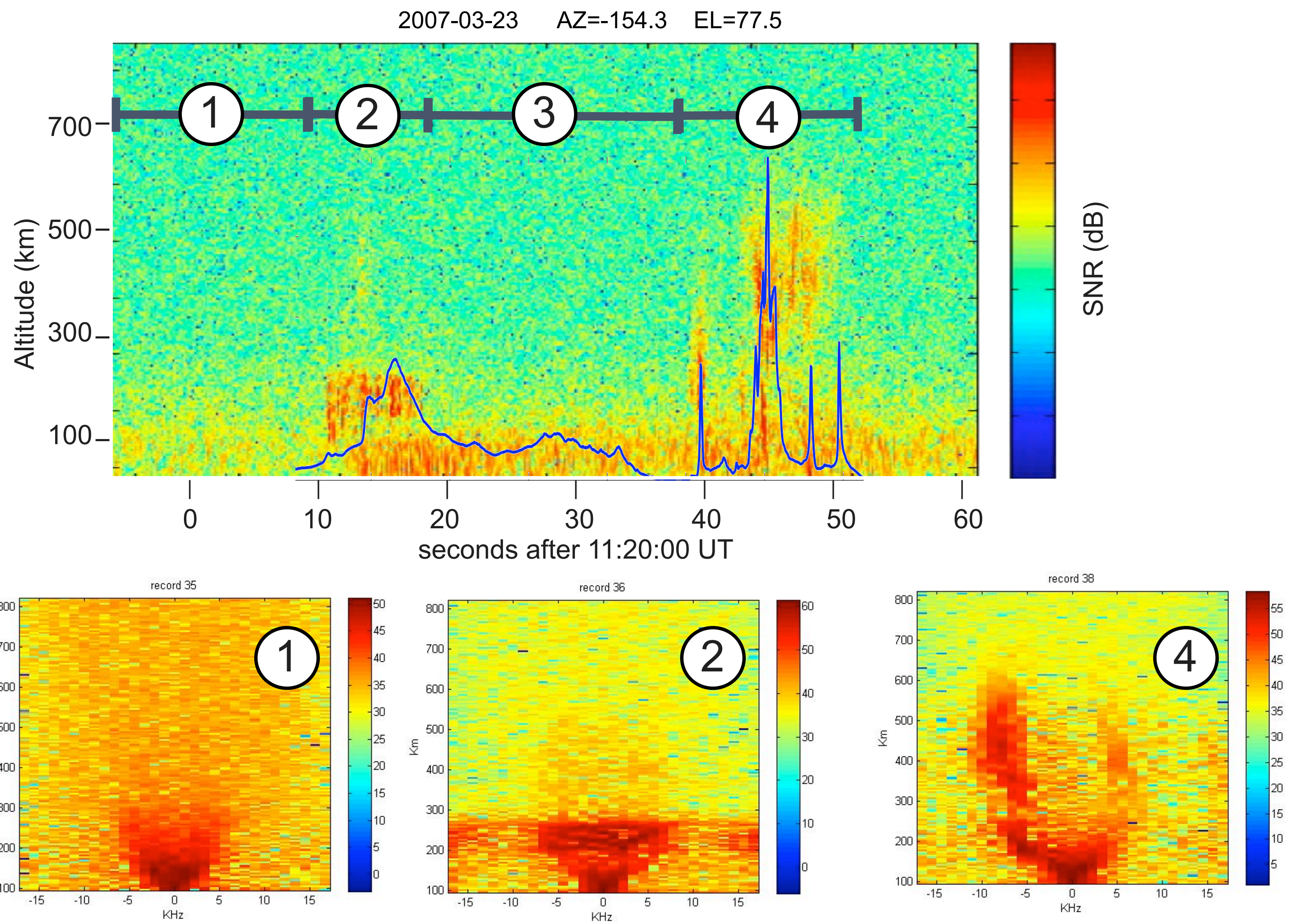

Stromme et al., AGU Fall Meeting, 2007

RISR: Resolute Bay ISR

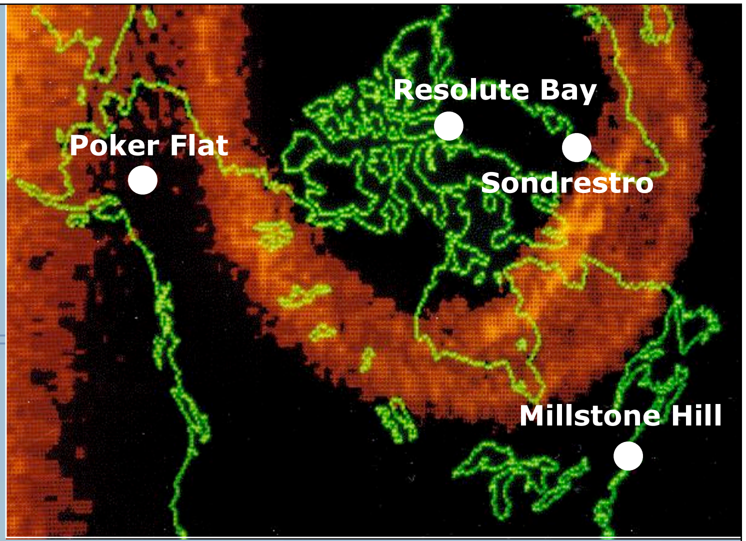

RISR: An initial look at the polar cap ionosphere

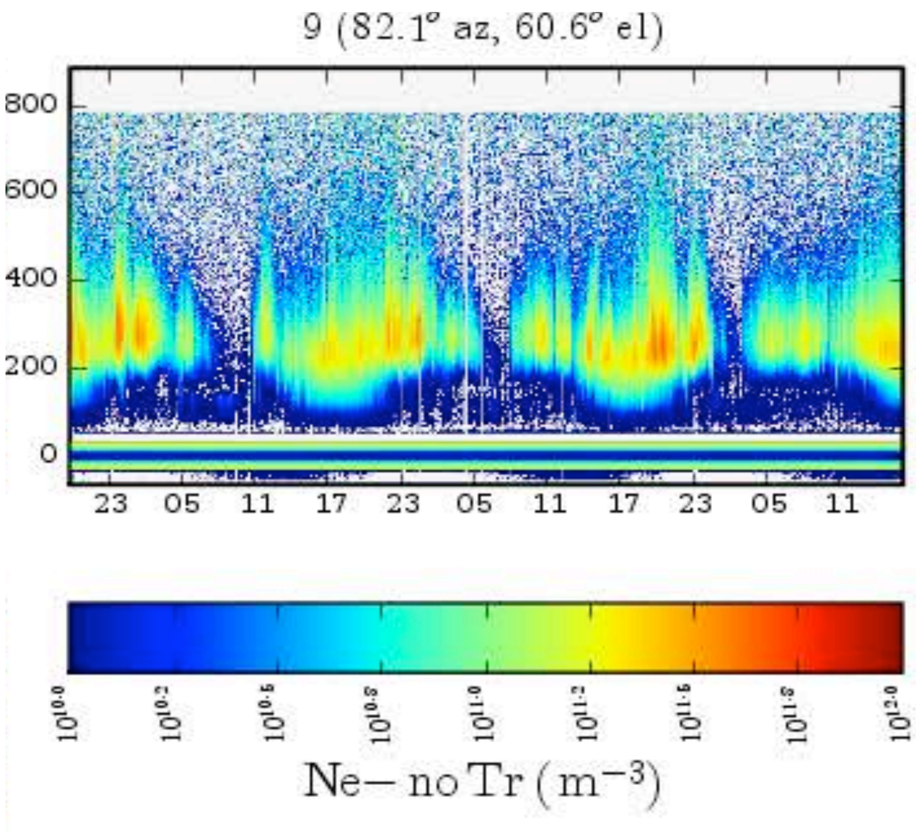

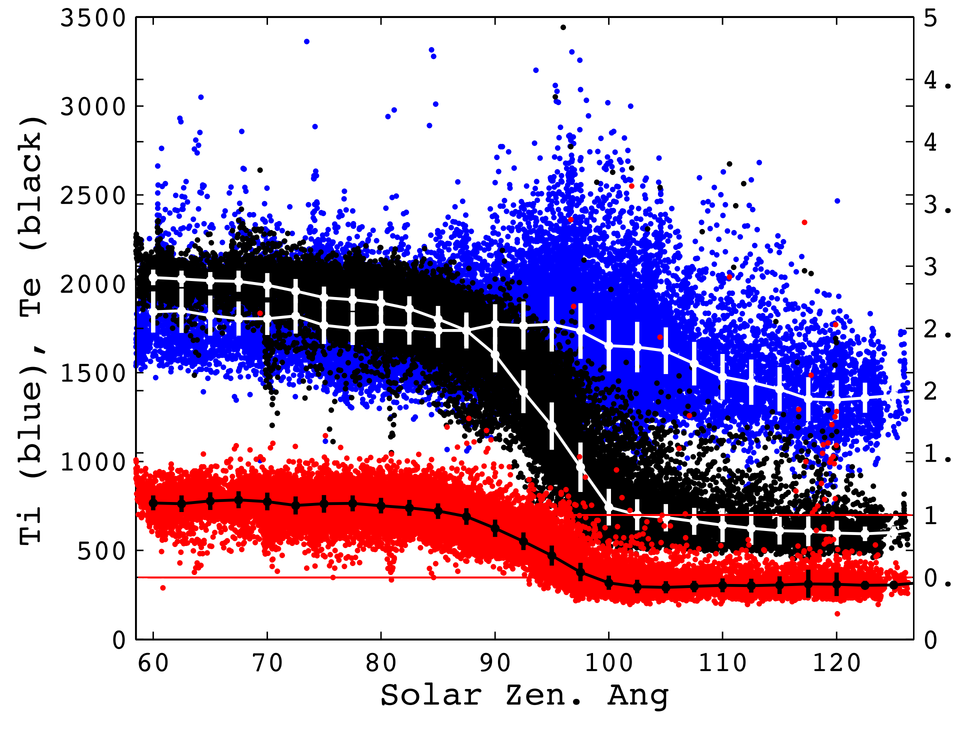

Nicolls , Heinselman, Kelly, et al., Unpublished

What has yet to be done

- Radar mode development
- Assimilation with ancillary diagnostics
- Conjugate studies with satellites and rockets

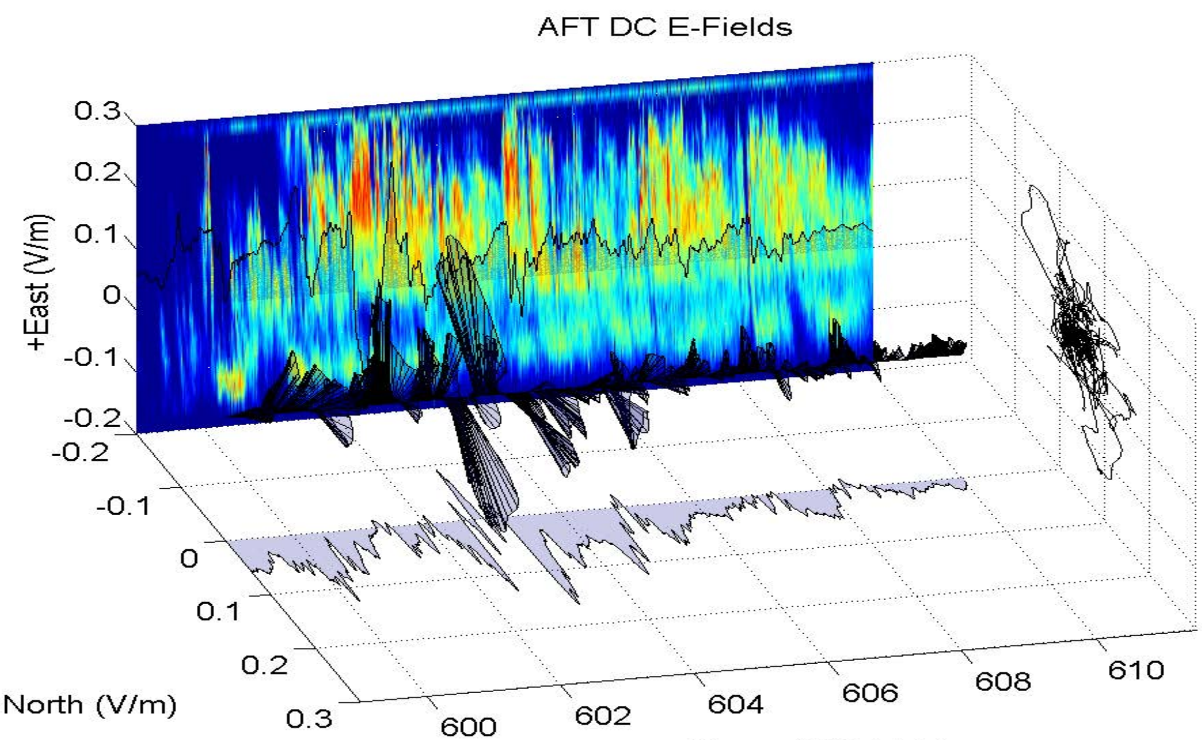

Lynch et al. 2010 (in press)

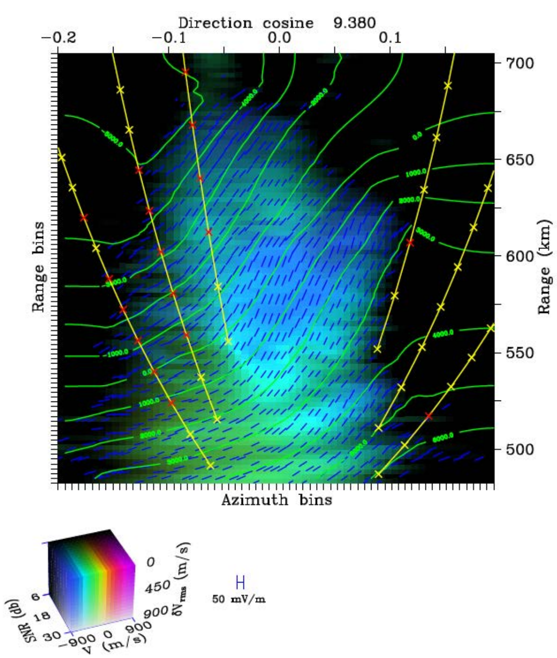

Hysell et al, Ann. Geophys. 2008


THE END